Materials Research Proceedings 31 (2023) 117-127 https://doi.org/10.21741/9781644902592-13

Static response of FGM shell using refined higher-order shear and normal deformation theory

Sumit S. Kolapkar[1,2,a *], Atteshamuddin S. Sayyad[2,b]

[1]Research Scholar, Department of Civil Engineering, Sanjivani College of Engineering, Savitribai Phule Pune University, Kopargaon-423603, Maharashtra, India

[2]Department of Structural Engineering, Sanjivani College of Engineering, Savitribai Phule Pune University, Kopargaon-423603, Maharashtra, India

[a]sumitkolapkar@gmail.com[*], [b]attu_sayyad@yahoo.co.in

Keywords: Static Response, FGM Shell, Higher-Order Shear And Normal Deformation Theory

Abstract. In the present study, a static response of functionally graded plate and spherical shells is investigated using higher-order trigonometric shear and normal deformation theory. A need of the shear correction factor is obviated and the effect of actual cross-sectional warping has been considered to get the realistic behaviour of transverse shear stresses across the thickness of the shell. The Navier solution technique has been used to analyse the simply-supported boundary conditions of the shell. To verify the theory, the numerical results obtained using the present theory are compared with other higher-order shear deformation theories available in the literature. The numerical results are obtained with and without considering the effects of transverse normal strain (ε_z).

Introduction

The development of functionally graded materials (FGM) has broad applications in the fields of off-shore structures, aerospace, rocket casing, nuclear mining, power plants, etc. It consists of two distinct materials that behave separately to obtain specific desired features depending on the application for which FGM is used. These materials have quite varied engineering properties. It is a substance whose physical characteristics, such as its density and coefficient of thermal expansion, gradually change along a single (usually along its thickness) or multiple directions. A material's gradation in a specific direction improves properties such as thermal conductivity, corrosion resistance, hardness, stiffness, weldability, etc. The most often used FGM composites are made of ceramic and metal, where the former offers strong thermal insulation and corrosion resistance, and the latter offers good fracture and toughness coupled with weldability. Classical shell theory [1] neglects the effects of transverse shear stresses therefore provides inaccurate results of displacements and stresses for thick plates and shells. Mindlin [2] has developed a first order shear deformation theory which considers the effect of transverse shear stresses for thin and moderately thick plates and shells, but it does not satisfy realistic shear stress conditions at the top and the bottom surfaces of the shell. This necessitated the development of higher-order refined shear deformation theories which consider the effects of both transverse shear and normal deformations. A new sinusoidal shear deformation theory is developed by Thai and Vo [3] for the bending, buckling, and vibration analysis of FGM plates. Shyang and Yen [4] investigated the elastic behaviour of moderately thick, rectangular, simply-supported FGM plates. Mantari et al. [5] used the Carrera unified formulation for the static analysis of FGM single-layer and multi-layered sandwich plates including the trigonometric, exponential, and hyperbolic type functions in the displacement fields. Response of FGM plate under thermo-mechanical loading is investigated by Bhandari and Purohit [6, 7] for varied boundary conditions and aspect ratios. The impact of the

Materials Research Proceedings 31 (2023) 117-127 https://doi.org/10.21741/9781644902592-13

shear correction factor on the static behaviour of porous FGM plates is evaluated by Mota et al. [8]. With the use of two refined higher-order models, Punera and Kant [9] examined the elastostatics behaviour of laminated and FGM sandwich cylindrical shells. For the thermal analysis of FGM plates, Swaminathan and Sangeetha [10] explored several modelling methodologies and its solutions, using the four variable refined plate theory, Zidi et al. [11] investigated the bending response of a FGM plate supported by an elastic foundation and exposed to hygrothermal and mechanical loadings. A literature on the stress, vibration, and buckling analysis of FGM plates is reviewed by Swaminathan et al. [12]. The effectiveness of a novel fifth-order shear and normal deformation theories for the static and dynamic responses of sandwich FGM plates and shells is examined by Shinde and Sayyad [13, 14]. A bending response is studied for FG beam using semi-analytical and by shear deformation theory under transverse loading conditions by Yadav et al. [15]. A static and free vibration analysis of doubly-curved FGM shells using different types of higher-order shell theories via unified formulation is presented by Sayyad and Ghugal [16]. Analysis of FG sandwich plates using a fifth order shear deformation theory is carried out by Thai et al. [17]. For the bending analysis of FGM plates based on the four variable plate theory, Demirhan and Taskin [18] employed the Levy solution. The observations that need further study are based on the literature review that is done.

1. Laminated composite and FGM plates' mechanical analyses have been extensively studied in the literature. However, there is very little study on mechanical analysis of FGM shells in the entire body of literature.
2. Researchers are paying more attention to cylindrical shell analyses. There is, however, a dearth of information on mechanical analysis of doubly curved FGM shells.
3. Many theories available in the literature ignores the effects of transverse normal strain on the analysis of FGM shells which plays an important role for the accurate structural analysis of FGM shells under mechanical/environmental loading conditions.

Methodology

The analysis in the current study takes into account a single layer FGM shell that is simply-supported at edges as shown in Fig. 1. It has curved dimensions of "*a*" and "*b*" along *x*-*y* directions and "*h*" is the thickness of the shell along *z*-direction. The principle radii of curvature of the mid-plane along the *x*-*y* directions are R_1 and R_2, respectively. The distance between the shell's top and bottom surfaces from the mid-plane surface is ($z = -h/2$) and ($z = +h/2$), respectively. A transverse load of intensity $q(x,y)$ is applied to the top surface of the shell.

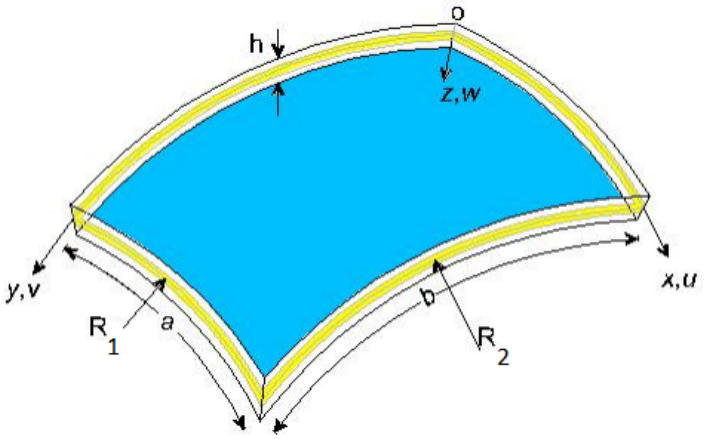

Fig. 1 Geometry and coordinate systems of FGM shell

The FGM used to create the shell has gradations of material properties in the direction of thickness i.e. z-direction according to the power-law. Following is the simple form of power law.

$$E(z) = E_m + (E_c - E_m)V_f. \tag{1}$$

where, $E(z)$ is the value of modulus of elasticity at any point of the shell in the z-direction; E_m and E_c are the modulus of elasticity of metal and ceramic, respectively; V_f is the volume fraction which is given as

$$V_f = \left(0.5 + \frac{z}{h}\right)^p. \tag{2}$$

where p is the power law factor. When $p = 0$ shell is fully ceramic whereas for $p = \infty$ it is fully metallic.

Formulation

The displacement field of the present higher-order trigonometric shear and normal deformation theory is written as

$$\begin{aligned} U(x,y,z) &= \left(1 + \tfrac{z}{R_1}\right)u_0(x,y) - z\frac{\partial w_0}{\partial x} + \frac{h}{\pi}\sin\left(\frac{\pi z}{h}\right)\theta_x, \\ V(x,y,z) &= \left(1 + \tfrac{z}{R_2}\right)v_0(x,y) - z\frac{\partial w_0}{\partial y} + \frac{h}{\pi}\sin\left(\frac{\pi z}{h}\right)\theta_y, \\ W(x,y,z) &= w_0(x,y) + C_1\cos\left(\frac{\pi z}{h}\right)\theta_z. \end{aligned} \tag{3}$$

where, U, V, W are the displacements of any point in the x-, y-, and z- directions respectively; $u_0(x,y), v_0(x,y)$ and $w_0(x,y)$ are the displacement of a point on the mid-plane in x-, y-, and z-directions respectively; $\theta_x(x,y), \theta_y(x,y)$ and $\theta_z(x,y)$ are the shear slopes. $\left(\frac{h}{\pi} sin \frac{\pi z}{h}\right)$ is the trigonometric function associated with the transverse shear strain. $(1 + z/R_1)$ and $(1 + z/R_2)$ are the Lame's constant; and C_1 is the arbitrary constant account for the consideration of effects of transverse normal strain. When C_1=0, $\varepsilon_z = 0$ and when C_1 =1, $\varepsilon_z \neq 0$. Using linear theory of elasticity, the normal strain and shear strain components are obtained.

$$\begin{aligned} \varepsilon_x &= \frac{\partial u_0}{\partial x} - z\frac{\partial^2 w_0}{\partial x^2} + f(z)\frac{\partial \theta_x}{\partial x} + \frac{w_0}{R_1} + C_1\frac{f'(z)\theta_z}{R_1}, \\ \varepsilon_y &= \frac{\partial v_0}{\partial y} - z\frac{\partial^2 w_0}{\partial y^2} + f(z)\frac{\partial \theta_y}{\partial y} + \frac{w_0}{R_2} + C_1\frac{f'(z)\theta_z}{R_2}, \\ \varepsilon_z &= C_1 f''(z)\theta_z, \\ \gamma_{xy} &= \frac{\partial u_0}{\partial y} + \frac{\partial v_0}{\partial x} - 2z\frac{\partial^2 w_0}{\partial x \partial y} + f(z)\frac{\partial \theta_x}{\partial y} + f(z)\frac{\partial \theta_y}{\partial x}, \\ \gamma_{xz} &= f'(z)\theta_x + C_1 f'(z)\frac{\partial \theta_z}{\partial x}, \\ \gamma_{yz} &= f'(z)\theta_y + C_1 f'(z)\frac{\partial \theta_z}{\partial y}. \end{aligned} \tag{4}$$

where

$$f(z) = \frac{h}{\pi}\left(\sin\frac{\pi z}{h}\right), f'(z) = \cos\left(\frac{\pi z}{h}\right), f''(z) = -\sin\left(\frac{\pi z}{h}\right)\frac{\pi}{h}. \tag{5}$$

Stress components associated with the strain components mentioned in Eq. (4) are obtained using the following stress-strain relationship which is also called as generalized Hooke's law.

$$\begin{Bmatrix}\sigma_x\\ \sigma_y\\ \sigma_z\\ \tau_{xy}\\ \tau_{xz}\\ \tau_{yz}\end{Bmatrix}=\begin{bmatrix}Q_{11} & Q_{12} & Q_{13} & 0 & 0 & 0\\ Q_{12} & Q_{22} & Q_{23} & 0 & 0 & 0\\ Q_{13} & Q_{23} & Q_{33} & 0 & 0 & 0\\ 0 & 0 & 0 & Q_{66} & 0 & 0\\ 0 & 0 & 0 & 0 & Q_{44} & 0\\ 0 & 0 & 0 & 0 & 0 & Q_{55}\end{bmatrix}\begin{Bmatrix}\varepsilon_x\\ \varepsilon_y\\ \varepsilon_z\\ \gamma_{xy}\\ \gamma_{xz}\\ \gamma_{yz}\end{Bmatrix}. \tag{6}$$

where

$$\begin{aligned} Q_{11}=Q_{22}=Q_{33}&=\frac{E(z)(1-\mu)}{(1+\mu)(1-2\mu)},\\ Q_{12}=Q_{13}=Q_{21}=Q_{23}=Q_{31}=Q_{32}&=\frac{E(z)\mu}{(1+\mu)(1-2\mu)},\\ Q_{44}=Q_{55}=Q_{66}&=\frac{E(z)}{2(1+\mu)}. \end{aligned} \tag{7}$$

where, $(\sigma_x,\sigma_y,\sigma_z,\tau_{xy},\tau_{xz},\tau_{yz})$are the normal and shear stress components, $(\varepsilon_x,\varepsilon_y,\varepsilon_z,\gamma_{xy},\gamma_{yz},\gamma_{xz})$are the normal and shear strain components, $(Q_{11},Q_{12},Q_{13},Q_{22},Q_{23},Q_{33},Q_{44},Q_{55},Q_{66})$are the reduced stiffness matrix components, $E(z)$ is the modulus of elasticity and μ is the Poisson's ratio. The principle of virtual work is used to derive the governing differential equations and boundary conditions associated with the present theory.

$$\int_0^a\int_0^b\int_{-h/2}^{+h/2}\left(\sigma_x\delta\varepsilon_x+\sigma_y\delta\varepsilon_y+\sigma_z\delta\varepsilon_z+\tau_{xy}\delta\gamma_{xy}+\tau_{xz}\delta\gamma_{xz}+\tau_{yz}\delta\gamma_{yz}\right)dxdydz=\int_0^a\int_0^b q\delta w dxdy. \tag{8}$$

Substituting Eqs. (4) - (6) in Eq. (8), performing triple integration by parts and collecting the coefficients of unknown variables, the following six governing differential equations are derived.

$$\begin{aligned} \delta u_0&:\frac{\partial N_x}{\partial x}+\frac{\partial N_{xy}}{\partial y}=0,\\ \delta v_0&:\frac{\partial N_y}{\partial y}+\frac{\partial N_{xy}}{\partial x}=0,\\ \delta w_0&:\frac{\partial^2 M_x^b}{\partial x^2}+\frac{\partial^2 M_y^b}{\partial y^2}+2\frac{\partial^2 M_{xy}^b}{\partial x\partial y}-\frac{N_x}{R_1}-\frac{N_y}{R_2}+q=0,\\ \delta\theta_x&:\frac{\partial M_x^s}{\partial x}+\frac{\partial M_{xy}^s}{\partial y}-Q_x^S=0,\\ \delta\theta_y&:\frac{\partial M_y^s}{\partial y}+\frac{\partial M_{xy}^s}{\partial x}-Q_y^S=0,\\ \delta\theta_z&:\frac{\partial Q_x^S}{\partial x}+\frac{\partial Q_y^S}{\partial y}-\frac{S_x}{R_1}-\frac{S_y}{R_2}-S^S=0. \end{aligned} \tag{9}$$

where

$$\begin{aligned}\left(N_x, N_y, N_{xy}, M_x^b, M_y^b, M_{xy}^b\right) &= \int_{-h/2}^{+h/2}\left(\sigma_x, \sigma_y, \tau_{xy}, z\sigma_x, z\sigma_y, z\tau_{xy}\right) dz,\\ \left(M_x^s, M_y^s, M_{xy}^s\right) &= \int_{-h/2}^{+h/2} f(z)\left(\sigma_x, \sigma_y, \tau_{xy}\right) dz,\\ \left(S_x, S_y, Q_x^S, Q_y^S\right) &= \int_{-h/2}^{+h/2} f'(z)\left(\sigma_x, \sigma_y, \tau_{xz}, \tau_{yz}\right) dz,\\ S^S &= \int_{-h/2}^{+h/2} f''(z)\sigma_z\, dz.\end{aligned} \tag{10}$$

where the in-plane force resultants are (N_x, N_y, N_{xy}); the shear force resultants are (S_x, S_y, Q_x^s, Q_y^s, S^s); the resultant bending moments are (M_x^b, M_y^b, M_{xy}^b); and the resultant shear moments are (M_x^s, M_y^s, M_{xy}^s). The superscript "b" stands for traditional bending effects, while the superscript "s" stands for shear effects. After substitution of stress resultant expressions from Eq. (10) into six governing equation stated in Eq. (9), one can derive governing equations in terms of unknown variables.

$$\begin{aligned}\delta u_0: A_{11}\left(\frac{\partial^2 u_0}{\partial x^2}+\frac{1}{R_1}\frac{\partial w_0}{\partial x}\right) - B_{11}\frac{\partial^3 w_0}{\partial x^3} + C_{11}\frac{\partial^2 \theta_x}{\partial x^2} + A_{12}\left(\frac{\partial^2 v_0}{\partial x\partial y}+\frac{1}{R_2}\frac{\partial w_0}{\partial x}\right) - B_{12}\frac{\partial^3 w_0}{\partial x\partial y^2} + C_{12}\frac{\partial^2 \theta_y}{\partial x\partial y}\\ +\left(\frac{F_{11}}{R_1}+\frac{F_{12}}{R_2}\right)\frac{\partial \theta_z}{\partial x}C_1 + D_{13}\frac{\partial \theta_z}{\partial x}C_1 + A_{66}\left(\frac{\partial^2 u_0}{\partial y^2}+\frac{\partial^2 v_0}{\partial x\partial y}\right) - 2B_{66}\frac{\partial^3 w_0}{\partial x\partial y^2} + C_{66}\left(\frac{\partial^2 \theta_x}{\partial y^2}+\frac{\partial^2 \theta_y}{\partial x\partial y}\right) = 0.\end{aligned} \tag{11}$$

$$\begin{aligned}\delta v_0: A_{12}\left(\frac{\partial^2 u_0}{\partial x\partial y}+\frac{1}{R_1}\frac{\partial w_0}{\partial y}\right) - B_{12}\frac{\partial^3 w_0}{\partial x^2\partial y} + C_{12}\frac{\partial^2 \theta_x}{\partial x\partial y} + A_{22}\left(\frac{\partial^2 v_0}{\partial y^2}+\frac{1}{R_2}\frac{\partial w_0}{\partial y}\right) + \left(\frac{F_{12}}{R_1}+\frac{F_{22}}{R_2}\right)\frac{\partial \theta_z}{\partial y}C_1\\ -B_{22}\frac{\partial^3 w_0}{\partial y^3} + C_{22}\frac{\partial^2 \theta_y}{\partial y^2} + D_{23}\frac{\partial \theta_z}{\partial y}C_1 + A_{66}\left(\frac{\partial^2 u_0}{\partial x\partial y}+\frac{\partial^2 v_0}{\partial x^2}\right) - 2B_{66}\frac{\partial^3 w_0}{\partial x^2\partial y} + C_{66}\left(\frac{\partial^2 \theta_x}{\partial x\partial y}+\frac{\partial^2 \theta_y}{\partial x^2}\right) = 0.\end{aligned} \tag{12}$$

$$\begin{aligned}\delta w_0: B_{11}\left(\frac{\partial^3 u_0}{\partial x^3}+\frac{1}{R_1}\frac{\partial^2 w_0}{\partial x^2}\right) - H_{11}\frac{\partial^4 w_0}{\partial x^4} + I_{11}\frac{\partial^3 \theta_x}{\partial x^3} + \left(\frac{J_{11}}{R_1}+\frac{J_{12}}{R_2}\right)C_1\frac{\partial^2 \theta_z}{\partial x^2} + B_{12}\left(\frac{\partial^3 v_0}{\partial x^2\partial y}+\frac{1}{R_2}\frac{\partial^2 w_0}{\partial x^2}\right)\\ -H_{12}\frac{\partial^4 w_0}{\partial x^2\partial y^2} + I_{12}\frac{\partial^3 \theta_y}{\partial x^2\partial y} + K_{13}\frac{\partial^2 \theta_z}{\partial x^2}C_1 + B_{12}\left(\frac{\partial^3 u_0}{\partial x\partial y^2}+\frac{1}{R_1}\frac{\partial^2 w_0}{\partial y^2}\right) - H_{12}\frac{\partial^4 w_0}{\partial x^2\partial y^2} + I_{12}\frac{\partial^3 \theta_x}{\partial x\partial y^2} +\\ \left(\frac{J_{12}}{R_1}+\frac{J_{22}}{R_2}\right)C_1\frac{\partial^2 \theta_z}{\partial y^2} + B_{22}\left(\frac{\partial^3 v_0}{\partial y^3}+\frac{1}{R_2}\frac{\partial^2 w_0}{\partial y^2}\right) - H_{22}\frac{\partial^4 w_0}{\partial y^4} + I_{22}\frac{\partial^3 \theta_y}{\partial y^3} + K_{23}\frac{\partial^2 \theta_z}{\partial y^2}C_1\\ +2B_{66}\left(\frac{\partial^3 u_0}{\partial x\partial y^2}+\frac{\partial^3 v_0}{\partial x^2\partial y}\right) - 4H_{66}\frac{\partial^4 w_0}{\partial x^2\partial y^2} + 2I_{66}\left(\frac{\partial^3 \theta_x}{\partial x\partial y^2}+\frac{\partial^3 \theta_y}{\partial x^2\partial y}\right) - \frac{A_{11}}{R_1}\left(\frac{\partial u_0}{\partial x}+\frac{w_0}{R_1}\right) + \frac{B_{11}}{R_1}\frac{\partial^2 w_0}{\partial x^2}\\ -\frac{C_{11}}{R_1}\frac{\partial \theta_x}{\partial x} - \frac{1}{R_1}\left(\frac{F_{11}}{R_1}+\frac{F_{12}}{R_2}\right)C_1\theta_z - \frac{A_{12}}{R_1}\left(\frac{\partial v_0}{\partial y}+\frac{w_0}{R_2}\right) + \frac{B_{12}}{R_1}\frac{\partial^2 w_0}{\partial y^2} - \frac{C_{12}}{R_1}\frac{\partial \theta_y}{\partial y} - \frac{D_{13}}{R_1}C_1\theta_z - \frac{A_{12}}{R_2}\left(\frac{\partial u_0}{\partial x}+\frac{w_0}{R_1}\right)\\ +\frac{B_{12}}{R_2}\frac{\partial^2 w_0}{\partial x^2} - \frac{C_{12}}{R_2}\frac{\partial \theta_x}{\partial x} - \frac{1}{R_2}\left(\frac{F_{12}}{R_1}+\frac{F_{22}}{R_2}\right)C_1\theta_z - \frac{A_{22}}{R_2}\left(\frac{\partial v_0}{\partial y}+\frac{w_0}{R_2}\right) + \frac{B_{22}}{R_2}\frac{\partial^2 w_0}{\partial y^2} - \frac{C_{22}}{R_2}\frac{\partial \theta_y}{\partial y} - \frac{D_{23}}{R_2}C_1\theta_z = -q.\end{aligned} \tag{13}$$

$$\begin{aligned}\delta\theta_x: C_{11}\left(\frac{\partial^2 u_0}{\partial x^2}+\frac{1}{R_1}\frac{\partial w_0}{\partial x}\right) - I_{11}\frac{\partial^3 w_0}{\partial x^3} + L_{11}\frac{\partial^2 \theta_x}{\partial x^2} + C_{12}\left(\frac{\partial^2 v_0}{\partial x\partial y}+\frac{1}{R_2}\frac{\partial w_0}{\partial x}\right) - I_{12}\frac{\partial^3 w_0}{\partial x\partial y^2}\\ +\left(\frac{M_{11}}{R_1}+\frac{M_{12}}{R_2}\right)\frac{\partial \theta_z}{\partial x}C_1 + L_{12}\frac{\partial^2 \theta_y}{\partial x\partial y} + N_{13}\frac{\partial \theta_z}{\partial x}C_1 + C_{66}\left(\frac{\partial^2 u_0}{\partial y^2}+\frac{\partial^2 v_0}{\partial x\partial y}\right) - 2I_{66}\frac{\partial^3 w_0}{\partial x\partial y^2} +\\ L_{66}\left(\frac{\partial^2 \theta_x}{\partial y^2}+\frac{\partial^2 \theta_y}{\partial x\partial y}\right) - O_{55}\theta_x - O_{55}\frac{\partial \theta_z}{\partial x}C_1 = 0.\end{aligned} \tag{14}$$

$$\begin{aligned}\delta\theta_y: C_{21}\left(\frac{\partial^2 u_0}{\partial x\partial y}+\frac{1}{R_1}\frac{\partial w_0}{\partial y}\right) - I_{21}\frac{\partial^3 w_0}{\partial x^2\partial y} + L_{21}\frac{\partial^2 \theta_x}{\partial x\partial y} + C_{22}\left(\frac{\partial^2 v_0}{\partial y^2}+\frac{1}{R_2}\frac{\partial w_0}{\partial y}\right) - I_{22}\frac{\partial^3 w_0}{\partial y^3}\\ +\left(\frac{M_{21}}{R_1}+\frac{M_{22}}{R_2}\right)\frac{\partial \theta_z}{\partial y}C_1 + L_{22}\frac{\partial^2 \theta_y}{\partial y^2} + N_{23}\frac{\partial \theta_z}{\partial y}C_1 + C_{66}\left(\frac{\partial^2 u_0}{\partial x\partial y}+\frac{\partial^2 v_0}{\partial x^2}\right)\\ -2I_{66}\frac{\partial^3 w_0}{\partial x^2\partial y} + L_{66}\left(\frac{\partial^2 \theta_x}{\partial x\partial y}+\frac{\partial^2 \theta_y}{\partial x^2}\right) - O_{44}\theta_y - O_{44}\frac{\partial \theta_z}{\partial y}C_1 = 0.\end{aligned} \tag{15}$$

$$\delta\theta_z: O_{55}\left(\frac{\partial\theta_x}{\partial x}C_1+\frac{\partial^2\theta_z}{\partial x^2}C_1^2\right)+O_{44}\left(\frac{\partial\theta_y}{\partial y}C_1+\frac{\partial^2\theta_z}{\partial y^2}C_1^2\right)-\frac{F_{11}}{R_1}C_1\left(\frac{\partial u_0}{\partial x}+\frac{w_0}{R_1}\right)+\frac{J_{11}}{R_1}C_1\frac{\partial^2 w_0}{\partial x^2}$$
$$-\frac{M_{11}}{R_1}\frac{\partial\theta_x}{\partial x}C_1-\frac{F_{12}}{R_1}C_1\left(\frac{\partial v_0}{\partial y}+\frac{w_0}{R_2}\right)+\frac{J_{12}}{R_1}C_1\frac{\partial^2 w_0}{\partial y^2}-\frac{1}{R_1}\left(\frac{O_{11}}{R_1}+\frac{O_{12}}{R_2}\right)C_1^2\theta_z-\frac{M_{12}}{R_1}\frac{\partial\theta_y}{\partial y}C_1$$
$$-\frac{P_{13}}{R_1}C_1^2\theta_z-\frac{F_{12}}{R_2}C_1\left(\frac{\partial u_0}{\partial x}+\frac{w_0}{R_1}\right)+\frac{J_{12}}{R_2}C_1\frac{\partial^2 w_0}{\partial x^2}-\frac{M_{12}}{R_2}\frac{\partial\theta_x}{\partial x}C_1-\frac{F_{22}}{R_2}C_1\left(\frac{\partial v_0}{\partial y}+\frac{w_0}{R_2}\right)+\frac{J_{22}}{R_2}C_1\frac{\partial^2 w_0}{\partial y^2} \quad (16)$$
$$-\frac{1}{R_2}\left(\frac{O_{12}}{R_1}+\frac{O_{22}}{R_2}\right)C_1^2\theta_z-\frac{M_{22}}{R_2}\frac{\partial\theta_y}{\partial y}C_1-\frac{P_{23}}{R_2}C_1^2\theta_z-D_{13}C_1\left(\frac{\partial u_0}{\partial x}+\frac{w_0}{R_1}\right)+K_{13}C_1\frac{\partial^2 w_0}{\partial x^2}-N_{13}\frac{\partial\theta_x}{\partial x}C_1$$
$$-D_{23}C_1\left(\frac{\partial v_0}{\partial y}+\frac{w_0}{R_2}\right)+K_{23}C_1\frac{\partial^2 w_0}{\partial y^2}-\left(\frac{P_{13}}{R_1}+\frac{P_{23}}{R_2}\right)C_1^2\theta_z-N_{23}\frac{\partial\theta_y}{\partial y}C_1-S_{33}C_1^2\theta_z=0.$$

where

$$\left(A_{ij},B_{ij},C_{ij},D_{ij},F_{ij}\right)=Q_{ij}\int_{-h/2}^{+h/2}[1,z,f(z),f''(z),f'(z)]dz\,,$$
$$\left(H_{ij},I_{ij},J_{ij},K_{ij},L_{ij}\right)=Q_{ij}\int_{-h/2}^{+h/2}[z^2,f(z)z,f'(z)z,f''(z)z,f(z)^2]dz\,, \quad (17)$$
$$\left(M_{ij},N_{ij},O_{ij},P_{ij},S_{ij}\right)=Q_{ij}\int_{-h/2}^{+h/2}[f'(z)f(z),f''(z)f(z),f'(z)^2,f''(z)f'(z),f''(z)^2]dz.$$

The Navier Solution

The closed-form semi-analytical solution for the static analysis of FGM shell for a simply-supported boundary condition can be obtained by using the Navier solution technique. Following are the simply supported boundary conditions associated with the present theory.
At the edge $x = 0$ and $x = a$

$$v_0 = w_0 = M_x^b = M_x^s = N_x = 0 \quad (18)$$

At the edge $y = 0$ and $y = b$

$$u_0 = w_0 = M_y^b = M_y^s = N_y = 0 \quad (19)$$

Therefore, the unknown variable according to the Navier technique in the form of double trigonometric series satisfying boundary conditions stated in Eqs. (18) and (19) can be expressed as

$$u_0=u_{mn}\cos\alpha x\sin\beta y,\ v_0=v_{mn}\sin\alpha x\cos\beta y,\ w_0=w_{mn}\sin\alpha x\sin\beta y,$$
$$\theta_x=\theta_{x_{mn}}\cos\alpha x\sin\beta y,\ \theta_y=\theta_{y_{mn}}\sin\alpha x\cos\beta y,\ \theta_z=\theta_{z_{mn}}\sin\alpha x\sin\beta y. \quad (20)$$

where $\alpha=m\pi/a$, $\beta=n\pi/b$, and $\left(u_{mn},v_{mn},w_{mn},\theta_{xmn},\theta_{ymn},\theta_{zmn}\right)$ are the unknown coefficients. The uniform mechanical load acting on the top surface of the shell is also expressed in double trigonometric series as follows.

$$q(x,y)=q_{mn}\sin\alpha x\sin\beta y. \quad (21)$$

where, q_{mn} is Fourier coefficient of load; for sinusoidal load $q_{mn} = q_0$ where q_0 is the maximum intensity of the load with m =1 and n = 1. Substituting Eqs. (20) and (21) in to Eqs. (11) – (16) leads to the six simultaneous equations which can we written in the following matrix form.

$$[K]\{\Delta\}=\{f\}. \quad (22)$$

where matrices $[K]$, $\{f\}$ and $\{\Delta\}$ are the stiffness matrix, the force vector and the vector of unknowns, respectively.

Materials Research Proceedings 31 (2023) 117-127 https://doi.org/10.21741/9781644902592-13

Numerical Results and Discussion

In this section, the accuracy of the present higher-order trigonometric shear and normal deformation theory is verified by applying it for the static analysis to FGM plates and shells. The FGM shell is made up from the following materials.

$$E_c = 380\,GPa, E_m = 70\,GPa, \text{and } \mu = 0.3$$

where E_c and E_m are the modulus of elasticity for ceramic (alumina) and metal (aluminium) respectively.

Following non-dimensional forms are used to present the numerical values of displacements and stresses.

$$\overline{w}\left(\frac{a}{2},\frac{b}{2},0\right) = \frac{10E_c h^3}{q_0 a^4}, w^*\left(\frac{a}{2},\frac{b}{2},0\right) = \frac{100E_0 h^3}{q_0 a^4}, \overline{\sigma}_x\left(\frac{a}{2},\frac{b}{2},-\frac{h}{2}\right) = \frac{h}{q_0 a}\sigma_x, \overline{\tau}_{xz}\left(0,\frac{b}{2},\frac{z}{h}\right) = \frac{h}{q_0 a}\overline{\tau}_{xz}. \quad (23)$$

For a single layer FGM plate and FGM spherical shell, the transverse displacement, in-plane, and transverse shear stresses are calculated with and without considering the effects of transverse normal strain. The FGM plate and FGM spherical shell results are shown here for a range of R/a ratios and for an a/h value of 10. The results obtained are contrasted with those of Shinde and Sayyad [14], Thai et al. [17], and Demirhan and Taskin [18]. Table 1 shows the comparison of displacements and stresses for FGM plate under sinusoidal loading with those presented by Shinde and Sayyad [14], Thai et al. [17], and Demirhan and Taskin [18]. Table 1 show that the transverse displacements increase whereas stresses are decreases with increase in the power-law index which is the effect of decrease in stiffness of material with increase in the power-law index. Fig. 2 shows through-the-thickness distributions of stresses in FGM plate. Table 2 shows the effects power law factor and radius of curvature on the dimensionless transverse displacement of FGM spherical shell under sinusoidal load. Table 2 reveals that the increase in radius of curvature and the power-law index increase the non-dimensional displacements and stresses in FGM spherical shell under the action of transverse sinusoidal load. Fig. 3 shows distribution of stresses through-the-thickness of the spherical shell.

Table 1 *Comparison of non-dimensional transverse displacements and stresses in FGM plate*

p	Theory	$\bar{w}$	$\bar{\sigma}_x$ (h/3)	$\bar{\tau}_{xz}$ (h/6)
1	Present ($\varepsilon_z \neq 0$)	0.5680	1.4158	0.2613
	Present ($\varepsilon_z = 0$)	0.5889	1.4893	0.2621
	Shinde and Sayyad [14] ($\varepsilon_z \neq 0$)	0.5695	1.4588	0.2607
	Thai et al. [17] ($\varepsilon_z = 0$)	0.5875	1.5062	0.2510
	Demirhan and Taskin [18] ($\varepsilon_z = 0$)	0.5889	1.4894	0.2622
	Thai et al. [17] ($\varepsilon_z = 0$)	0.5890	1.4898	0.2599
2	Present ($\varepsilon_z \neq 0$)	0.7198	1.3041	0.2754
	Present ($\varepsilon_z = 0$)	0.7573	1.3953	0.2763
	Shinde and Sayyad [14] ($\varepsilon_z \neq 0$)	0.7225	1.4588	0.2763
	Thai et al. [17] ($\varepsilon_z = 0$)	0.7570	1.5062	0.2510
	Demirhan and Taskin [18] ($\varepsilon_z = 0$)	0.7573	1.4894	0.2622
	Thai et al. [17] ($\varepsilon_z = 0$)	0.7573	1.3960	0.2721
4	Present ($\varepsilon_z \neq 0$)	0.8402	1.0801	0.2572
	Present ($\varepsilon_z = 0$)	0.8818	1.1782	0.2580
	Shinde and Sayyad [14] ($\varepsilon_z \neq 0$)	0.8429	1.1456	0.2630
	Thai et al. [17] ($\varepsilon_z = 0$)	0.8823	1.1985	0.2362
	Demirhan and Taskin [18] ($\varepsilon_z = 0$)	0.8819	1.1783	0.2580
	Thai et al. [17] ($\varepsilon_z = 0$)	0.8815	1.1794	0.2519
8	Present ($\varepsilon_z \neq 0$)	0.9431	0.8634	0.2114
	Present ($\varepsilon_z = 0$)	0.9750	0.9463	0.2120
	Shinde and Sayyad [14] ($\varepsilon_z \neq 0$)	0.9466	0.9088	0.2145
	Thai et al. [17] ($\varepsilon_z = 0$)	0.9738	0.9687	0.2262
	Demirhan and Taskin [18] ($\varepsilon_z = 0$)	0.9750	0.9466	0.2121
	Thai et al. [17] ($\varepsilon_z = 0$)	0.9747	0/9477	0.2087

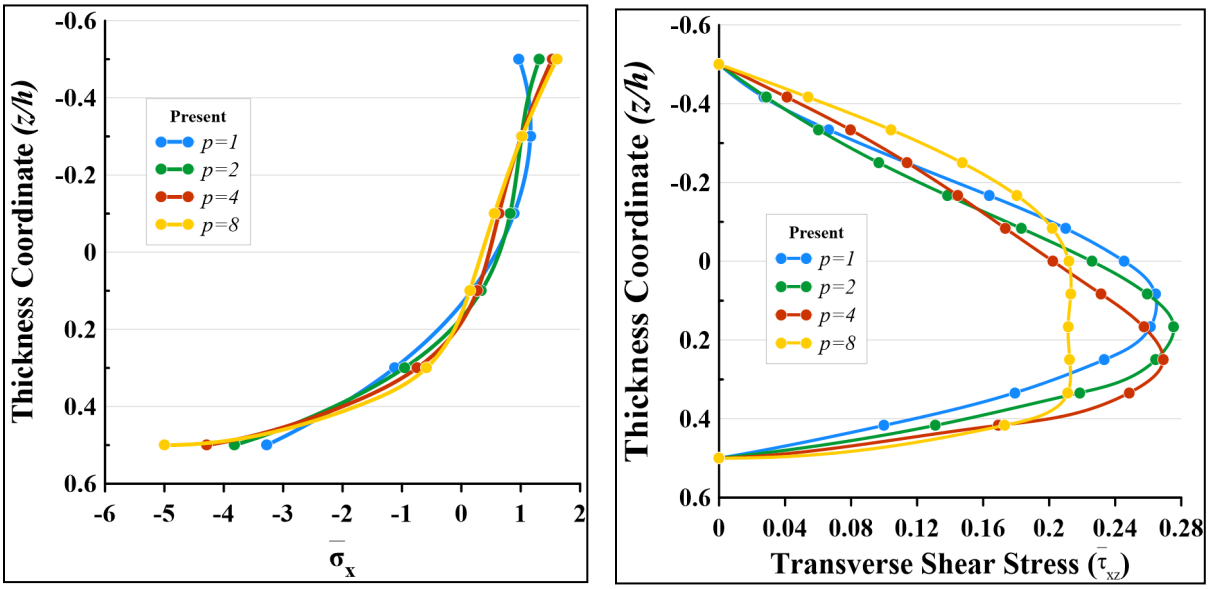

Fig. 2 *Variation of in-plane normal stresses and transverse shear stresses with respect to thickness coordinate for FGM plate at various power law index.*

Table 2 *Effects of radii of curvature and various power law factors on a non-dimensional transverse displacement and stresses in FGM spherical shell.*

		$C_1=1$ $(\varepsilon_z \neq 0)$			$C_1=0(\varepsilon_z = 0)$		
p	***R/a***	w^*	$\bar{\sigma}_x$	$\bar{\tau}_{xz}$	w^*	$\bar{\sigma}_x$	$\bar{\tau}_{xz}$
0	1	0.182285	0.8867	0.059227	0.196709	0.877621	0.062162
	2	0.426848	1.616985	0.136448	0.447698	1.5721	0.141477
	5	0.683527	2.161396	0.217494	0.696549	2.048913	0.220116
	10	0.747757	2.210737	0.237775	0.756631	2.081884	0.239102
	20	0.765746	2.185615	0.243455	0.773307	2.054303	0.244372
	50	0.770939	2.153269	0.245095	0.778108	2.022706	0.245889
	100	0.770939	2.139642	0.245331	0.778799	2.009705	0.246107
1	1	0.333162	1.340047	0.054467	0.345392	1.344237	0.059081
	2	0.818613	2.534497	0.138501	0.827979	2.435844	0.141629
	5	1.345933	3.434034	0.233552	1.360064	3.225955	0.232645
	10	1.467366	3.479844	0.256964	1.497545	3.267515	0.256162
	20	1.494501	3.410171	0.26295	1.536371	3.206274	0.262803
	50	1.497965	3.33761	0.264315	1.547605	3.141506	0.264725
	100	1.496925	3.308512	0.264385	1.549224	3.115356	0.265001
2	1	0.436394	1.661697	0.057442	0.447408	1.660349	0.062031
	2	1.062913	3.088568	0.146551	1.069408	2.952679	0.148269
	5	1.722104	4.084018	0.244961	1.751018	3.836549	0.242771
	10	1.867198	4.097459	0.268509	1.926424	3.854851	0.26709
	20	1.897397	3.996052	0.274366	1.975908	3.766159	0.273951
	50	1.899644	3.900158	0.275612	1.990222	3.68	0.275935
	100	1.897695	3.862666	0.275638	1.992284	3.645959	0.276221
4	1	0.558303	2.093204	0.06188	0.571133	2.08663	0.066412
	2	1.307231	3.711913	0.151393	1.314225	3.552994	0.152819
	5	2.033347	4.674429	0.242421	2.067377	4.410728	0.240396
	10	2.184533	4.629893	0.263082	2.251721	4.376198	0.261832
	20	2.215168	4.496298	0.268138	2.303061	4.257186	0.267802
	50	2.21703	4.380945	0.269192	2.317858	4.152421	0.269522
	100	2.214852	4.336984	0.269206	2.319988	4.112156	0.26977
8	1	0.677125	2.620321	0.054154	0.697486	2.62067	0.058081
	2	1.524411	4.474527	0.125934	1.536758	4.314154	0.127968
	5	2.293287	5.459686	0.193726	2.317603	5.18519	0.19299
	10	2.450173	5.382528	0.208615	2.498998	5.116218	0.208095
	20	2.483345	5.227416	0.21229	2.548872	4.976183	0.212248
	50	2.486733	5.097692	0.213098	2.563196	4.858044	0.213441
	100	2.485059	5.048693	0.213129	2.565255	4.813208	0.213613

Conclusions

In the current study, the static response of FGM plate and shell is studied using refined higher-order trigonometric shear and normal deformation theory. The currently used theory yields realistic boundary condition at the top and the bottom surfaces of the shell. The Navier technique has been used to calculate transverse displacements and stresses for FGM plates and spherical shell under the action of sinusoidal load. The obtained results are compared with previously published results. It is concluded that, the present results of static analysis of FGM plate and shell shows a good agreement with the previously published results when the effects of transverse normal strain is

considered. The other theories available in the literature overestimate the results due to neglecting the effects of transverse normal strain.

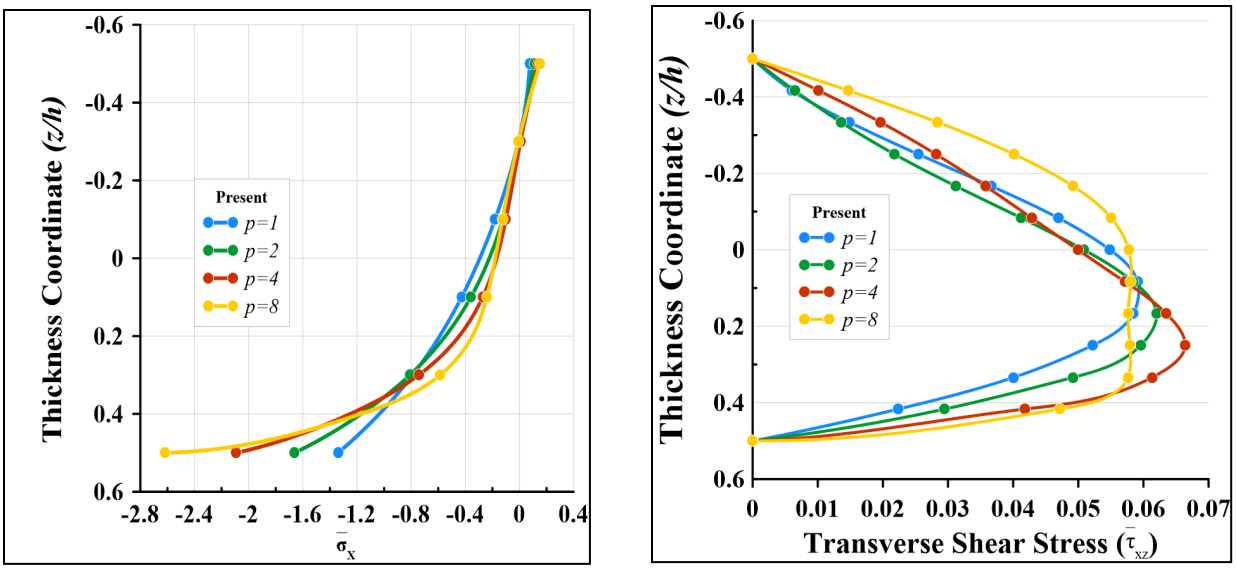

Fig. 3. *Variation of in-plane normal stresses and transverse shear stresses with respect to thickness coordinate for FGM spherical shell at various power law index (R/a = 1,* $\boldsymbol{\varepsilon_z \neq 0}$*).*

References

[1] G. Kirchhoff, Über das Gleichgewicht und die Bewegung, J Reine Angew Math. 40 (1850) 51-88. https://doi.org/10.1515/crll.1850.40.51

[2] R. D. Mindlin, Influence of Rotatory Inertia and Shear on Flexural Motions of Isotropic, Elastic Plates, J. Appl. Mech. vol. 18, no. 1(Mar. 1951) 31-38. doi: 10.1115/1.4010217. https://doi.org/10.1115/1.4010217

[3] H. T. Thai and T. P. Vo, A new sinusoidal shear deformation theory for bending, buckling, and vibration of functionally graded plates, Appl. Math. Model. vol. 37, no. 5 (2013) 3269-3281. doi: 10.1016/j.apm.2012.08.008. https://doi.org/10.1016/j.apm.2012.08.008

[4] S. H. Chi and Y. L. Chung, Mechanical behavior of functionally graded material plates under transverse load-Part I: Analysis, Int. J. Solids Struct. vol. 43, no. 13 (2006) 3657-3674. doi: 10.1016/j.ijsolstr.2005.04.011. https://doi.org/10.1016/j.ijsolstr.2005.04.011

[5] J. L. Mantari, I. A. Ramos, E. Carrera, and M. Petrolo, Static analysis of functionally graded plates using new non-polynomial displacement fields via Carrera Unified Formulation, Compos. Part B Eng. 89 (2016) 127-142. doi: 10.1016/j.compositesb.2015.11.025. https://doi.org/10.1016/j.compositesb.2015.11.025

[6] M. Bhandari and K. Purohit, Response of Functionally Graded Material Plate under Thermomechanical Load Subjected to Various Boundary Conditions, Int. J. Met. 2015 (2015) 1-16. doi: 10.1155/2015/416824. https://doi.org/10.1155/2015/416824

[7] M. Bhandari and K. Purohit, Static Response of Functionally Graded Material Plate under Transverse Load for Varying Aspect Ratio, Int. J. Met. 2014 (2014) 1-11. doi: 10.1155/2014/980563. https://doi.org/10.1155/2014/980563

[8] A. F. Mota, M. A. R. Loja, J. I. Barbosa, and J. A. Rodrigues, Porous Functionally Graded Plates: An Assessment of the Influence of Shear Correction Factor on Static Behavior, Math.

Comput. Appl. vol. 25, no. 2 (2020) 1-26. doi: 10.3390/mca25020025. https://doi.org/10.3390/mca25020025

[9] D. Punera and T. Kant, Elastostatics of laminated and functionally graded sandwich cylindrical shells with two refined higher order models, Compos. Struct. vol. 182, no. January (2017) 505-523. doi: 10.1016/j.compstruct.2017.09.051. https://doi.org/10.1016/j.compstruct.2017.09.051

[10] K. Swaminathan and D. M. Sangeetha, Thermal analysis of FGM plates - A critical review of various modeling techniques and solution methods, Compos. Struct. 160 (2017) 43-60. doi: 10.1016/j.compstruct.2016.10.047. https://doi.org/10.1016/j.compstruct.2016.10.047

[11] M. Zidi, A. Tounsi, M. S. A. Houari, E. A. Adda Bedia, and O. Anwar Bég, Bending analysis of FGM plates under hygro-thermo-mechanical loading using a four variable refined plate theory, Aerosp. Sci. Technol. vol. 34, no. 1 (2014) 24-34. doi: 10.1016/j.ast.2014.02.001. https://doi.org/10.1016/j.ast.2014.02.001

[12] K. Swaminathan, D. T. Naveenkumar, A. M. Zenkour, and E. Carrera, Stress, vibration and buckling analyses of FGM plates-A state-of-the-art review, Compos. Struct. 120 (2015) 10-31. doi: 10.1016/j.compstruct.2014.09.070. https://doi.org/10.1016/j.compstruct.2014.09.070

[13] B. M. Shinde and A. S. Sayyad, A new higher order shear and normal deformation theory for FGM sandwich shells, Compos. Struct. 280 (2022) 1-25. doi: 10.1016/j.compstruct.2021.114865. https://doi.org/10.1016/j.compstruct.2021.114865

[14] B. M. Shinde and A. S. Sayyad, A new higher-order theory for the static and dynamic responses of sandwich FG plates, J. Comput. Appl. Mech. vol. 52, no. 1 (2021) 102-125. doi: 10.22059/JCAMECH.2020.313152.569.

[15] S. Yadav, S. Damse, S. Pendhari, K. Sangle, and A. S. Sayyad, Comparative studies between Semi-analytical and shear deformation theories for functionally graded beam under bending, Forces Mech. 8 (2022). 01-12. doi: 10.1016/j.finmec.2022.100111. https://doi.org/10.1016/j.finmec.2022.100111

[16] A. S. Sayyad and Y. M. Ghugal, Static and free vibration analysis of doubly-curved functionally graded material shells, Compos.Struct. 269 (2021) 1-17. doi:10.1016/j.compstruct.2021.114045. https://doi.org/10.1016/j.compstruct.2021.114045

[17] H.-T. Thai, T.-K. Nguyen, T. P. Vo, and J. Lee, Analysis of functionally graded sandwich plates using a new first-order shear deformation theory, Eur. J. Mech. - A/Solids. 45 (2014) 211-225. doi: 10.1016/j.euromechsol.2013.12.008. https://doi.org/10.1016/j.euromechsol.2013.12.008

[18] P. A. Demirhan and V. Taşkin, Static analysis of simply supported functionally graded sandwich plates by using four variable plate theory, Tek. Dergi/Technical J. Turkish Chamb. Civ. Eng. vol. 30, no. 2 (2019) 8987-9007. doi: 10.18400/tekderg.396672. https://doi.org/10.18400/tekderg.396672